Plant Physiol. (1969) 44, 881-885

Design, Calibration and Field Use of a Stomatal Diffusion Porometer

E. T. Kanemasu, G. W. Thurtell[1], and C. B. Tanner
University of Wisconsin, Madison, Wisconsin 53706

Received February 14, 1969.

Abstract. **Modifications of the design and calibration procedure of a diffusion porometer permit determinations of stomatal resistance which agree well with results obtained by leaf energy balance. The energy balance and the diffusion porometer measurements indicate that the boundary layer resistances of leaves in the field are substantially less than those predicted from heat transport formulas based on wind flow and leaf size.**

The flux of water vapor from leaves is determined by the difference in water vapor concentration between the substomatal cavities and the ambient air stream and the diffusive resistance in the pathway. The total diffusive resistance is the sum of the stomatal and boundary layer resistances. The stomatal resistance can be found when the boundary layer resistance is low from leaf energy balance, water vapor and temperature gradient measurements. The diffusion porometer measures the stomatal diffusion resistance directly (10, 11); other indirect methods are described by Slatyer (8) and Barrs (1).

The porometer design and calibration procedure suggested by Van Bavel *et al.* (10) does not provide a theoretical or an experimental linear relationship between the time lapse, Δt, and the resistance. With long calibration tubes (high resistance), a $(\Delta t)^{1/2}$ relation is found as theory predicts. Their diffusion porometer does not provide the flexibility of measuring low and high resistances within a time lapse, Δt, of 1 min, and the large opening of their vapor cup confines its use to broad-leaf plants. Their electronic circuit draws more current than necessary to operate the sensor; hence, frequent replacement of the 4 mercury batteries is required.

This paper describes design modifications of the diffusion porometer, discusses its calibration and temperature corrections, and compares the total resistance obtained from water balance of individual leaves under field conditions with the total resistance obtained from the porometer measurement of stomatal resistance and the energy balance measurement of the boundary layer resistance.

Design

Vapor Cup. The preferred geometry for a vapor cup design is a flat sensor forming an end to the cup. Since no flat humidity sensors with sufficiently rapid response were available, we used the same sensor as Van Bavel *et al.* (10) (Hygrosensor #4-4817. Hygrodynamics, Incorporated, 949 Selim Road, Silver Spring, Maryland 20910). However, we positioned it parallel to the evaporating surface in a hemicylinder formed by milling away part of an acrylic cylinder and cementing it over an opening cut into an acrylic baseplate (Fig. 1). A silicone rubber adhesive (Dow-Corning RTV732), applied at each end of the sensor holds the sensor in place. Inserts which contain various aperture shapes, appropriate to the type of leaf, fit into the opening in the baseplate. The insert is made of a linen-base phenolic plastic which allows the perforated shim stock to be epoxied onto the insert. The perforated shim stock (0.076-mm thick stainless steel with uniformly spaced 1-mm holes) provides protection to the humidity sensor and reduces convection. The shim stock resistance assures that the time lapse is about triple the time constant of the humidity sensor ($r_o \sim 15$ sec). A latex-foam pad (foot plaster), coated with a thin layer of RTV732, is positioned around the aperture and provides a seal between the baseplate and the leaf surface. An acrylic plate, which is fastened to the baseplate by a hinge, clamps the leaf against the latex-foam padding. A thermistor bead (General Electric #81B105) is placed

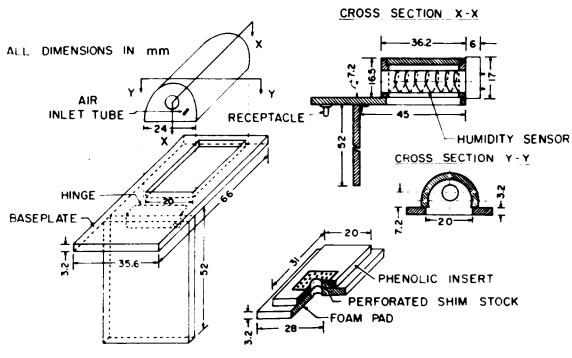

FIG. 1. Construction drawing of the vapor cup.

[1] Present address: Soils Department, University of Guelph, Guelph, Ontario.

next to the humidity sensor to measure the air temperature inside the cup. A 5-pin receptacle (Amphenol #223-1105) on the acrylic baseplate connects the sensor and thermistor to the measuring circuit.

Circuit. A multivibrator circuit (Fig. 2) provides a stable, square-wave voltage with a peak-to-peak amplitude of approximately 24 v a-c across the collectors of T_1 and T_2. The frequency is about 90 Hz. All resistors are 5 % except R_{10} which is 1 %. Two 6.75-volt mercury batteries (Mallory TR135R) supply 3.4 ma to the circuit; hence, the mercury batteries will last about 300 hr. A constant a-c voltage must be applied across the sensor to insure calibration stability. This is accomplished by adjusting to full scale (10 μa) with the variable resistor (R_8) when the sensor position is shorted.

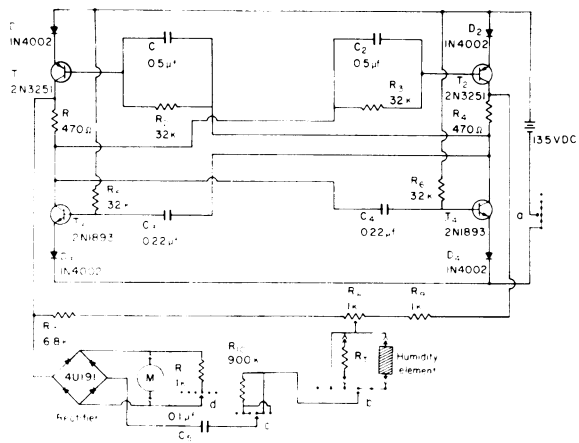

FIG. 2. Schematic of the porometer electronics.

The a-c current through the sensor is rectified and monitored with a microammeter, M (API Instruments #302). To prevent polarization damage, direct current through the sensor must be very small; this is insured with C_5. A 4-pole, 6-position, 2-wafer switch is used to turn on the circuit (pole a); determine the full-scale calibration, the temperature *via* the thermistor, or the humidity (pole b); switch R_{10} in series with the humidity sensor or thermistor (pole c); and shunt the meter with R_{11} (pole d).

By adjusting the circuit, the meter can operate over any portion of the sensor humidity range (Fig. 3). When measuring leaves with stomatal resistances less than about 5 sec cm^{-1}, the ammeter is shunted with R_{11}. The time lapse is measured for the ammeter reading to change from 2 to 10 μa which corresponds to a change in relative humidity from approximately 22.5 to 29 %. For stomatal resistances greater than 5 sec cm^{-1}, the ammeter is not shunted and R_{10} is shorted. The time lapse is measured for the ammeter reading to increase from 2 to 6 μa, which corresponds to a relative humidity change from approximately 18 to 20 %, and allows the measurement to be taken rapidly. The last position of the switch covers the same humidity range

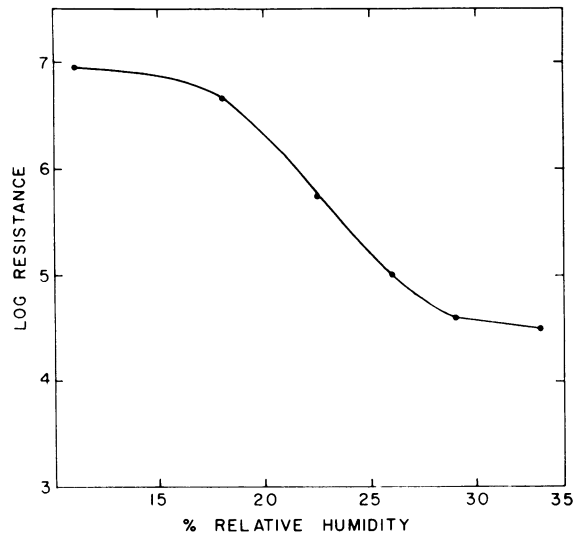

FIG. 3. Typical response curve of the narrow-range humidity sensor. Resistance in ohms.

(12–33 %) as the circuit suggested by Van Bavel *et al.* (10).

Calibration

Many small tubes obtained by drilling small holes in an acrylic plate, are used to simulate the stomatal resistance. The resistance is calculated by

$$r = L/\alpha = 4A(L_o + \frac{\pi d}{4})/\alpha n\pi d^2 \qquad (1)$$

where L is the effective diffusion path length, α is the diffusivity of water vapor in air, L_o is the actual length of each hole, A is the insert aperture area, n is the number of holes, and d is diameter of the holes. To correct for "end effects", $\pi d/4$ is added to the actual diffusion path of each tube. The vapor storage of these resistances is small so that steady-state vapor gradients are established quickly across the resistance.

High resistances are made by varying the number of 1-mm diameter holes and the thickness of the plates. To obtain consistent results, it is necessary to keep the total cross-sectional area of the holes ($n\pi d^2/4$) greater than 1/30 of the aperture area. Low resistances (< 4 sec cm^{-1}) are made by cutting holes of the same size as the aperture of the diffusion porometer in thin acrylic plates. These resistances are equal to the thickness of the plate divided by α.

To calibrate the porometer, the cup aperture is placed on an undrilled portion of the resistance plate and air is pumped into the cup through a column of silica gel with a hand-pumped rubber bulb. Then, the cup aperture is positioned over the holes of the acrylic resistance plate which is over a saturated blotter paper. Acrylic stops are mounted on the plates, facilitating rapid and proper placement of the cup. The time lapse for the meter reading to increase over the specified limits is measured with a stop watch.

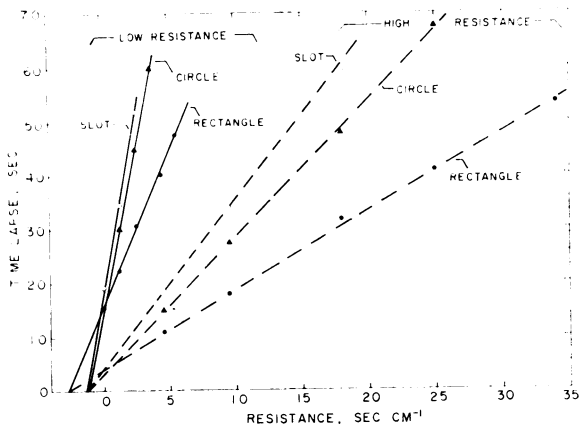

FIG. 4. Calibration curves using 3 aperture geometries. The solid curves were obtained with ammeter shunted (Fig. 2) and the dashed lines were obtained with ammeter not shunted.

Calibration curves for 3 different aperture geometries (Fig. 4)—a rectangle with an area of 2.90 cm^2, a narrow slot with an area of 1.11 cm^2 and a circle with an area of 1.27 cm^2—are shown in Fig. 4. Temperatures of the wet blotter surface and the air inside the cup were at 25°.

The stomatal resistance is calculated by the equation

$$r_s = r_o + \Delta t/S \qquad \text{(II)}$$

where Δt is the time lapse; S is the slope of the calibration curve and r_o is the diffusive resistance of the vapor cup which is taken as the intercept of the curve and the abscissa. The slope of calibration curve ($\Delta t/r$) is directly proportional to the amount of water vapor that diffuses into the cup and inversely proportional to the aperture area. Assuming that the total amount of water vapor diffusing into the cup remains constant when measuring between the same time lapse limits (microammeter end points), the ratio of the slopes of the calibration lines should be inversely proportional to the aperture areas. The agreement of the slope ratios of Fig. 4 and aperture areas is within 20 % at low slopes and about 5 % at high slopes.

A check on the porometer calibration was made by comparing ($r_s + r_o$) from the calibration curve with the total diffusive resistance calculated from the total amount of water vapor being transported during the time lapse and the vapor pressure gradient between the sensor and the vapor source. The water vapor that diffused into the cup was either adsorbed onto the sensor and cup walls or remained in the gas phase in the cup. The amount of water vapor adsorbed by the sensor and the walls of the cup was estimated by placing known volumes of air of known relative humidities in contact with the humidity sensor. A vapor cup without a sensor was equilibrated in a closed container over a saturated salt solution of known relative humidity. A second vapor cup containing a sensor was filled with drier air and the relative humidity was read. The 2 cup openings were covered with thin plastic sheets and after the cups were brought together, the plastic separations were removed and the equilibrium relative humidity was determined by another sensor reading. Two tests were run with initial relative humidities of 53 % and 75 % in the first chamber and with 17 % in the second chamber; the equilibrium relative humidities were 23 % and 30 %, respectively. Assuming that changes in adsorption of water vapor on the cup walls is negligible as compared with changes in storage in the humectant, we calculated for both trials that the sensor and the walls adsorbed about 66 % of the water vapor in the cup. From this storage and the time lapse, the total water vapor flux was calculated. The total diffusive resistance was then calculated from the vapor pressure gradient and the flux; the result agreed with equation I within 10 %.

The sensitivity of the porometer is inversely proportional to its aperture area, but sampling a large area may be desirable, necessitating a compromise. We have found, that we can repeat measurements on tobacco and bean leaves ($r_s \sim 1$ sec cm^{-1}) with the larger aperture within 0.5 sec error in the time lapse or with an error of about 0.3 sec cm^{-1}.

The tube-type (10) and pore-type calibration resistances are compared in Fig. 5 at a system temperature of 25°. The curve obtained with the tubes is linear when plotted as $\Delta t^{1/2}$, as predicted from diffusion theory. When the tube resistance is assumed proportional to its length errors arise. The tube- and pore-type resistances at a time lapse of 10 sec are 3 and 2 sec cm^{-1}, respectively, and at a time lapse of 90 sec, the tube- and pore-type resistances are 23 and 35 sec cm^{-1}, respectively.

Surface and air temperatures also affect the slope

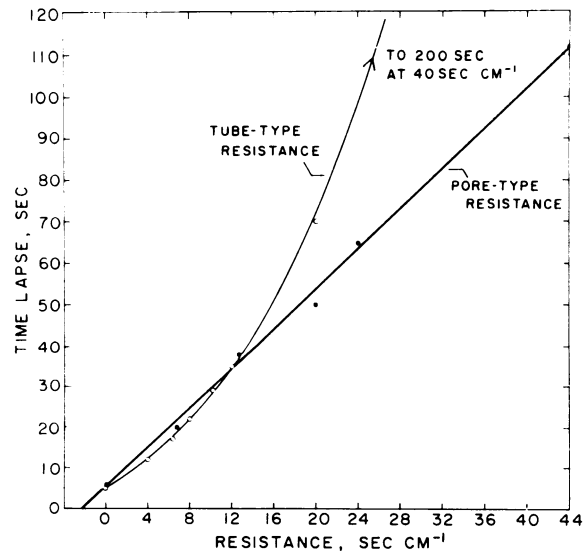

FIG. 5. Comparison of calibration curves obtained from tube-type and pore-type resistance elements.

of the calibration curve. These effects can be calculated from the vapor pressure gradient between the saturated surface and the air in the vapor cup and the amount of water vapor that must diffuse into the cup to result in a given change in relative humidity. The following equation applies:

$$S_2/S_1 = [(e_{s_1} - e_{a_1})/(e_{s_2} - e_{a_2})] \cdot [0.34\ (e_{a_2}^*/e_{a_1}^*) + 0.66] \quad \text{(III)}$$

where S_1 and S_2 are the respective slopes of the known and unknown calibration curves, e_{s_1} and e_{s_2} are the vapor pressures of the surface for the 2 calibration curves; e_{a_1} and e_{a_2} are the corresponding vapor pressures of the air inside the cup and are obtained from the air temperature and the relative humidity as indicated by the thermistor and humidity sensor; and $e_{a_1}^*$ and $e_{a_2}^*$ are the saturated vapor pressure at the air temperature at which the calibration curves were obtained. Calculated values using equation III predict the experimental values to within 5 %.

Field Tests

Individual Leaf Energy Balance. The energy balance of a leaf can be written as

$$R_n = E + H \quad \text{(IV)}$$

where R_n is the net radiation; E is the latent heat flux density and H is the sensible heat. All the terms in IV are based upon the total surface area of the leaf, *i.e.*, twice the plan area.

Although the net radiation can be obtained by summing all the separate radiation streams, we used a miniature Funk net radiometer (2). A view factor correction (3) for the leaf's background radiation and for the shadow the radiometer casts on the leaf is necessary to obtain the net radiation of the leaf in the absence of the radiometer. The sensible heat, H, can be obtained from IV, where R_n and E are measured. It is also equal to

$$H = \rho c_p (T_s - T_a)/r_x \quad \text{(V)}$$

where T_s is the temperature of leaf, T_a is the temperature of air, and r_x is the mean boundary layer resistance of the leaf to heat flow.

The evaporative flux density can be obtained directly with detached leaves in potometers (7) or as we have done by growing plants in pots and removing all leaves but one from the plant. The water loss from the known leaf area can be determined by sealing off evaporation from the soil and periodically weighing the pots. Also,

$$E = \rho c_p (e_s - e_a)/\gamma r_t \quad \text{(VI)}$$

where e_s is the vapor pressure of the substomatal cavity and is assumed to be the saturation vapor pressure at leaf temperature, e_a is the vapor pressure of the air outside the leaf boundary layer, ρ is the density of moist air, c_p is the specific heat of moist air, and γ is the psychrometric constant (mb/deg). The mean resistance, r_t, to vapor flow from a thin leaf is

$$\frac{2}{r_t} = \frac{1}{r_a + r_x} + \frac{1}{r_b + r_x} \quad \text{(VII)}$$

where r_a and r_b are the adaxial and abaxial stomatal diffusion resistances for vapor, and r_x is the boundary layer resistance for heat and water vapor. Since the r_x for heat and vapor differ about 15 %, an average for the two may be taken to represent either with small error. If free convection is an important part of the transfer relative to forced convection, the adaxial and abaxial r_x differ.

The measurements of T_s, T_a, the wet bulb depression of the air, R_n and E allow the determination of H, r_x and r_t. By solving the 3 equations, IV, V, and VI, the energy balance parameters obtained by the above method are listed for 10 separate analyses in table I. The test leaves were snap bean plants (*Phaseolus vulgaris* L., var. Bush Blue Lake) placed both in the shade and bright sunlight at different locations within a snap bean row.

The stomatal resistances, r_a and r_b, were measured with the diffusion porometer. The mean vapor diffusion resistance of the leaf on a total leaf area basis was calculated as in VII using the energy balance value of r_x. The stomatal resistances measured with the diffusion porometer represent an average of 2 or 3 determinations taken during the period of the energy balance measurements. We believe that the diffusion resistances obtained from the water balance, energy balance and stomatal porometer agree within

Table I. *Energy Balance Measurements of Snap Bean Plants* (Phaseolus vulgaris), *Computed Boundary Layer and Mean Vapor Diffusion Resistances From Energy Balance and Porometer Measurements*

Date	R_n	E	H	Air temp	Leaf temp	$(e_s - e_a)$	r_x (E.B.)	r_t (E.B.)	r_t (P)
		mly sec^{-1}			*deg*	*mb*		*sec/cm*	
July 19	11.1	1.2	9.9	23.0	26.6	19.7	0.10	7.0	5.9
July 19	2.80	1.0	1.8	23 0	23.2	10.7	0.03	4.2	4.2
July 20	4.94	4.6	0.34	25.0	25.5	15.7	0.40	1.5	3.0
July 22	12.0	2.63	9.37	24.9	28.0	24.7	0.10	4.0	4.5
July 22	11.5	3.8	7.7	24.0	26.0	15.0	0.07	1.7	2.3
July 26	5.68	1.08	4.60	22.2	23.2	12.0	0.06	4.7	4.2
July 26	—0.10	0.90	—1.0	22.2	20.8	8.1	0.40	3.8	3.4
Aug 2	14.5	4.38	10.12	29.5	29.9	27.2	0.01	2.6	2.5
Aug 6	3.43	1.30	2.13	31.2	32.6	10.2	0.20	3.3	2.6
Aug. 6	4.68	1.90	2.78	31.1	32.5	10.0	0.14	2.2	1.9

Table II. *Mean Boundary Layer Resistances Obtained From the Energy Balance and From Forced and Free Convection Equations*

Date	Wind speed	Forced r_x (H.T.)	Free r_x (H.T.)	Mixed r_x (H.T.)	r_x (E.B.)
	cm/sec		*sec/cm*		
July 19	144	0.8	4.6	0.68	0.10
July 19	100	1.0	9.4	0.90	0.03
July 20	25	2.0	7.5	1.60	0.40
July 22	225	0 7	4.5	0.60	0.10
July 22	105	1.0	5.3	0.84	0.07
July 26	34	1.8	6 0	1.40	0.06
July 26	36	1.8	5.8	1.38	0.40
Aug 2	140	0.8	8.0	0.72	0.01
Aug 6	56	1.4	5.8	1.13	0.20
Aug 6	70	1.3	5.8	1.06	0.14

the combined error of the measurements.

With additional measurements of leaf size and wind speed near the leaf (5), we can compare the r_x(E.B.) determined from the energy balance with r_x(H.T.) obtained from the standard heat transport theory (6, 9). The boundary layer resistances obtained from forced- and free-convection formulas were added in parallel to give the lowest estimate of the boundary layer resistance for mixed convection (table II). The mixed-convection boundary layer resistance, r_x(H.T.) is at least a factor of 5 greater than that obtained from the energy balance, r_x(E.B.). Hunt *et al.* (4) found similar results with sunflower leaves (*Helianthus annuus*) when the boundary layer resistance was computed from R_n, ΔT, Δe and r_s measurements (the stomatal resistance, r_s, was measured with a porometer). It is noted that while the equation used by Hunt *et al.* (4) is not correct in principle since they set $r_t = r_s + r_x$ rather than using VII, the results are realistic because r_x was small compared to r_s.

The absolute error associated with our measurements of r_x(E.B.) is small; the evaporation and net radiation are measured directly and errors can be estimated. Also using r_x(H.T.) and the sensible heat flux density, an unreasonable temperature gradient is calculated. The low boundary layer resistance found experimentally may be attributed to the scale of turbulence found under field conditions. to leaf flutter, and to the attitude of the leaf to the wind. An intensity of turbulence of 60 % is not uncommon in the free atmosphere. Standard heat transport formulas provide good results in wind tunnels where intensity of turbulence range from 0.1 to 6 % and a laminar boundary layer is formed over the surface.

Precautions. There are certain precautions that must be taken when using the instrument: A) condensation on the sensor must be avoided and the sensor should be stored in a desiccator when not in use, B) the sensor should be conditioned by repeated cycling from dry to moist after removing from desiccator, C) the leaf should be shaded for a few seconds before the measurement so that its temperature is stabilized near that in the porometer and the vapor cup should be shielded from sunlight. The leaf and sensor in many cases can be used in the operator's shadow. With shading, only the air temperature inside the cup must be measured to make the necessary temperature corrections to the calibration curve. It was found during field measurements on snap beans that there is no significant change in stomatal resistance when the vapor cup is left on the leaf for periods up to 15 to 20 min if the leaf-water potential is greater than about —9 bars. At leaf-water potentials less than about —10 bars, the stomatal resistance rapidly increases if the cup remains on the leaf for longer than 2 to 3 min.

Acknowledgments

Contribution from the Department of Soils, University of Wisconsin, Madison. Published with the permission of the Director of the Wisconsin Agricultural Experiment Station. This work was completed while the senior author was a CIC Fellow in Biometeorology, supported by Training Grant (2T1AP16) from National Center for Air Pollution Control, U.S.P.H.S., and partly supported by the Green Giant Company, Le Sueur, Minnesota and in part by USDA Hatch Funds. The authors gratefully acknowledge Mr. Austin A. Millar for his assistance in the field measurements.

Literature Cited

1. Barrs, H. D. 1968. Determination of water deficits in plant tissues. In: Water Deficits and Plant Growth. Vol. 1: Development, Control and Measurement. T. Kozlowski, ed. Academic Press, New York. p 235–368.
2. Funk, J. P. 1962. A net radiometer designed for optimum sensitivity and a ribbon thermopile used in a miniaturized version. J. Geophys. Res. 67: 2753–60.
3. Hamilton, D. C. and W. R. Morgan. 1952. Radiant-interchange configuration factors. NACA. Tech. Note 2836. 110 p.
4. Hunt, L. A., I. I. Impens, and E. R. Lemon. 1968. Estimates of the diffusion resistance of some large sunflower leaves in the field. Plant Physiol. 43: 522–26.
5. Kanemasu, E. T. and C. B. Tanner. 1968. A note on a heat transport anemometer. Bioscience 18: 327–29.
6. McAdams, W. H. 1954. Heat Transmission. Third Ed. McGraw-Hill, New York. 532 p.
7. Miller, P. C. and D. M. Gates. 1967. Transpiration resistance of plants. Am. Midland Naturalist 77: 77–85.
8. Slatyer, R. O. 1967. Plant-Water Relationships. Academic Press, New York. 336 p.
9. Thom, A. S. 1968. The exchange of momentum, mass, and heat between an artificial leaf and the airflow in a wind tunnel. Quart. J. Roy. Meteorol. Soc. 94: 44–55.
10. Van Bavel, C. H. M., F. S. Nakayama, and W. L. Ehrler. 1965. Measuring transpiration resistance of leaves. Plant Physiol. 40: 535–40.
11. Wallihan, E. F. 1964. Modification and use of an electric hygrometer for estimating relative stomatal apertures. Plant Physiol. 39: 86–90.